Available online at www.sciencedirect.com
SCIENCE DIRECT®
Sensors and Actuators A 111 (2004) 79–86
SENSORS AND ACTUATORS A PHYSICAL
www.elsevier.com/locate/sna

Water-activated disposable and long shelf life microbatteries☆

Firas Sammoura*, Ki Bang Lee, Liwei Lin

Berkeley Sensor and Actuator Center, Department of Mechanical Engineering, University of California at Berkeley, 1113 Etcheverry Hall, Berkeley, CA 94720-1740, USA

Received 1 February 2003

Abstract

Water-activated microbatteries with long shelf life have been demonstrated based on a one-mask micromachining process for the first time. Magnesium is used as the anode and silver chloride or cuprous chloride is used as the cathode in the prototype demonstration. Adding water or aqueous solutions activate the electrochemical reactions between the anode and cathode to release electricity. Experimentally, a maximum output voltage was measured at 1.65 V using silver chloride cathode and the maximum operation capacity has been demonstrated to be more than 1.86 mWh when an electrode area of 12 mm × 12 mm was used. As such, these microbatteries have great potential to be integrated with micro devices as the power sources for microsystems, such as disposable diagnostics and BioMEMS chips.

Keywords: Microbattery; Micropower; Disposable; Microsystem; Micromachine

1. Introduction

The field of MEMS is emerging as an important technology of the new millennium with the capability of creating complex, autonomous, and low cost engineering systems [1]. One critical issue to be addressed is the power sources for microsystems. Although some micro devices such as ink-jet printers may not need on-board energy supplies, remote and distributed systems such as smart dusts do need local power sources [2]. As more MEMS devices are integrated with electronic circuits, the development of micropower sources for microsystems becomes exigent and challenging [3]. A huge amount of research efforts have been focusing on micro power generation for the past decade by using micro combustion and fuel cells that utilize oxygen, hydrogen, or other fuels to target continuous power supply in the range of 10–100 W [4]. Others have investigated the possibility of fabricating low cost and high capacity solar cells [5]. However, these micro power sources commonly require complicated micromachining processes that hindered the possibility of an integration solution with MEMS for self-sustained microsystems.

Micro power sources meeting the operation lifetime of disposable devices are attractive in contrast to the long-operation, miniature power sources of micro internal combustion engines [6] or rechargeable, thin-film lithium micro batteries [7]. In our previous work, an on-demand, surface micromachined microbattery based on electrolytes of sulfuric acid and hydrogen peroxide was demonstrated but the corrosiveness of sulfuric acid prevented safe battery operation [8]. This work presents microbatteries that are activated by water for safe operation and long shelf life. Water can be pre-stored on the system or be obtained from test liquids, including body fluids or blood to activate the battery to power disposable microsystems. It is envisioned that these microbatteries can be integrated with disposable microsystems such as diagnostic devices, DNA analyses chips and other bio-medical applications. Fig. 1 shows a disposable integrated microsystem. The front side of the substrate might have power-consuming systems and the backside of the substrate might have the disposable battery. The activation water can be obtained internally from the pre-stored water reservoir, or externally from the environment or testing liquids.

2. Operation principle

Fig. 2 shows the operation principle of the microbatteries that use magnesium (Mg) as the anode on the top substrate, and silver chloride (AgCl) or cuprous chloride (CuCl) as the cathode on the bottom substrate. The two pieces are bonded together by an adhesive (instant glue) to create the

☆ A portion of this paper was presented at the 16th IEEE Micro Electro Mechanical Systems Conference, Kyoto, 19–23 January 2003.

* Corresponding author. Tel.: +1-510-642-8983; fax: +1-510-642-6163.
E-mail address: firas@me.berkeley.edu (F. Sammoura).

0924-4247/$ – see front matter © 2003 Elsevier B.V. All rights reserved.
doi:10.1016/j.sna.2003.10.020

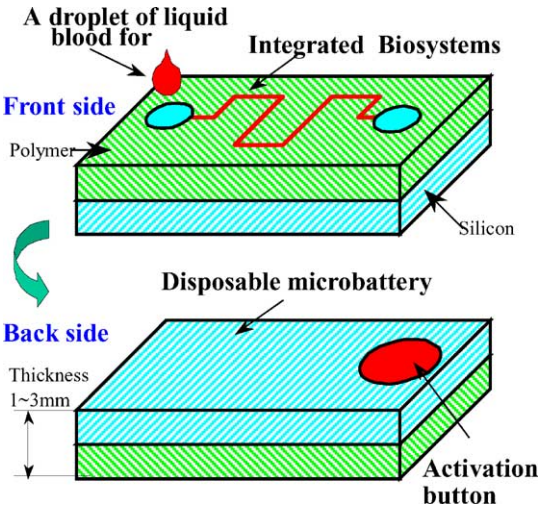

Fig. 1. Schematic of a disposable integrated system.

reaction chamber. Before water is added, there is no contact between these chemicals and no reaction is expected such that these microbatteries could have a long shelf-life. When water is added into the system, surface tension force drives it to fill the reaction chamber. Chemicals dissolve and react to produce electricity. The chemical reactions for the water-activated magnesium–silver chloride microbatteries at the anode (oxidation) and cathode (reduction) are represented as Eqs. (1) and (2), respectively [9]:

$$\mathrm{Mg} \rightarrow \mathrm{Mg^{2+}} + 2\mathrm{e^-} \tag{1}$$

$$2\mathrm{AgCl} + 2\mathrm{e^-} \rightarrow 2\mathrm{Ag} + 2\mathrm{Cl^-} \tag{2}$$

The overall reaction is:

$$\mathrm{Mg} + 2\mathrm{AgCl} \rightarrow \mathrm{MgCl_2} + 2\mathrm{Ag} \tag{3}$$

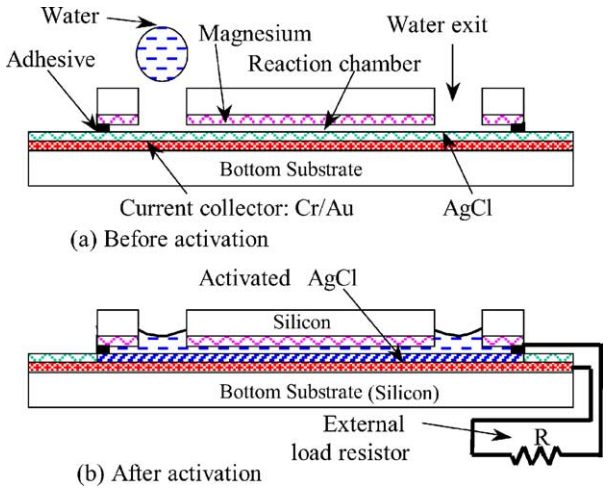

Fig. 2. Working principle of the water-activated microbattery. (a) Chemicals are not activated before putting water into the system. (b) Water activates silver chloride, and the microbattery becomes functional to supply power.

If cuprous chloride is used as the cathode, Eq. (2) is modified as:

$$2\mathrm{CuCl} + 2\mathrm{e^-} \rightarrow 2\mathrm{Cu} + 2\mathrm{Cl^-} \tag{4}$$

and the overall reaction is:

$$\mathrm{Mg} + 2\mathrm{CuCl} \rightarrow \mathrm{MgCl_2} + 2\mathrm{Cu} \tag{5}$$

A side reaction also occurs between the magnesium anode and the aqueous electrolyte, resulting in the formation of magnesium hydroxide, hydrogen gas and heat:

$$\mathrm{Mg} + 2\mathrm{H_2O} \rightarrow \mathrm{Mg(OH)_2} + \mathrm{H_2} \tag{6}$$

The formation of hydrogen bubbles creates a pumping action, which helps purging the insoluble magnesium hydroxide from the battery and might help the battery operation.

It is observed from Eqs. (1)–(5) that when electrons flow through the external load resistor, ions such as $\mathrm{Cl^-}$ and $\mathrm{Mg^{2+}}$ flow within the electrolyte. The theoretical voltage of a cell is a direct function of the anode and cathode materials. The potential of a cell can be calculated from the standard electrode potentials as the sum of the anode potential and the cathode potential [10]:

$$E^0 = E^0_{\mathrm{anode}} + E^0_{\mathrm{cathode}} \tag{7}$$

where E^0_{anode} and E^0_{cathode} are the anode oxidation potential and cathode reduction potential, respectively. The oxidation potential of a material is the negative value of its reduction potential. Using Eq. (7) and the data of Table 1, the standard potential of the Mg–AgCl microbattery is calculated as 2.585 V. Similarly, the theoretical voltage of the Mg–CuCl microbattery is calculated as 2.487 V.

The capacity of a cell, as defined by coulombs (C) or ampere hours (Ah), can be expressed as the total quantity of electricity involved in the electrochemical reaction. Theoretically, 1 g equiv. weight of a material that is defined as the molecular weight divided by the number of electrons involved in the reaction will deliver one Faraday (96,500 C) or 26.8 Ah. Hence, the theoretical electron capacity per unit weight, C_{el}, can be defined as follows:

$$C_{\mathrm{el}} = \sum \frac{nF}{\text{weight of reactants}} \tag{8}$$

where n is the number of electrons exchanged in the reaction and F is Faraday's number. Using Eq. (8) and the material properties from Table 1, the theoretical capacity per unit weight for the Mg–AgCl battery is 620.62 C/g

Table 1
Reduction potential and weights of chemicals

Material	Balanced-half reaction	Reduction potential, E^0 (V)	Weight (g/mol)
Mg	$\mathrm{Mg^{2+}} + 2e^- \rightarrow \mathrm{Mg\,(s)}$	−2.363	24.31
AgCl	$\mathrm{AgCl\,(s)} + e^- \rightarrow \mathrm{Ag(s)} + \mathrm{Cl^-}$	0.222	143.34
CuCl	$\mathrm{CuCl\,(s)} + e^- \rightarrow \mathrm{Cu\,(s)} + \mathrm{Cl^-}$	0.124	99.00

Table 2
Theoretical performance of Mg–CuCl and Mg–AgCl microbatteries

Anode	Cathode	E^0 (V)	C_{el} (Ah/g)	C_{en} (Wh/g)
Mg	AgCl	2.585	0.172	0.445
Mg	CuCl	2.487	0.241	0.599

or 0.172 Ah/g. Similarly, the theoretical capacity per unit weight for Mg–CuCl battery is 868.20 C/g or 0.241 Ah/g. The energy capacity per unit weight of batteries, C_{en}, is derived using $C_{en} = E^0 C_{el}$, where C_{en} is in Wh/g, E^0 is in Volt, and C_{el} is in Ah/g. Consequently, the energy capacities of the Mg–AgCl and Mg–CuCl batteries are 0.445 and 0.599 Wh/g, respectively. Table 2 summarizes the theoretical performance of the microbatteries presented in this paper.

3. Fabrication

The fabrication process is illustrated in Fig. 3. The water supply openings on the top substrate (Fig. 3(a)) are fabricated using the Deep Reactive Ion Etching (DRIE) process to etch through a 4-in. silicon wafer. A 15 μm-thick magnesium film is then deposited by using the evaporation process. It is expected that magnesium will also be deposited partially onto the sidewall. In Fig. 3(b), a Cr/Au layer of 200 Å/2000 Å is deposited using the sputtering process first as the current collector. Afterwards a layer of 20 μm-thick Ag layer is deposited by sputtering and then chlorinated to form the AgCl cathode. For CuCl, a 1.5 μm-thick CuCl is evaporated as the cathode. Alternatively, a 20 μm-thick CuCl is deposited by a screen-printing process as an inexpensive way to increase the amount of the chemicals for longer battery operation. Fig. 3(c) shows that both substrates are bonded to create a reaction chamber. The height of the chamber was controlled to be 50, 100, and 200 μm, by using various plastic spacers in the binding process. Moreover, microbatteries with different electrode areas have been fabricated, including 12 mm × 12 mm, 8 mm × 8 mm, 6 mm × 6 mm, and 4 mm × 4 mm. These microbatteries were tested experimentally to characterize the effects of geometrical variations. The fabrication process for microbatteries is compatible with most MEMS processes such that direct integration could be possible for disposable microsystems to have on-chip power sources. Fig. 4 shows an SEM of a fabricated microbattery. The electrode area of the microbattery is 8 mm × 8 mm. Fig. 5 is the close-up microphoto of the marker "A" in Fig. 5 showing chlorinated AgCl at the bottom, the 100 μm-high reaction chamber, and that Mg was deposited on the side wall of the top substrate.

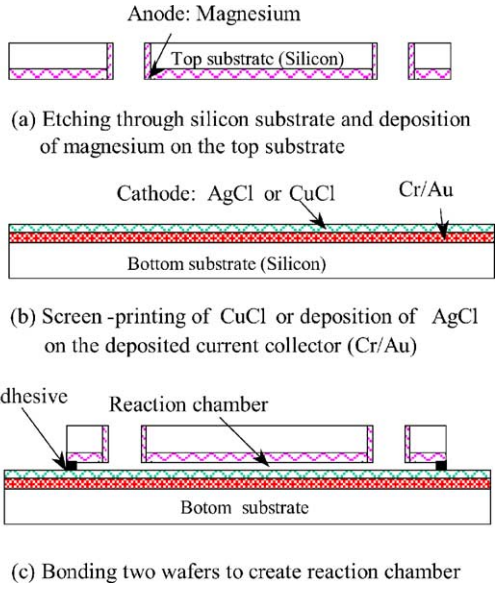

Fig. 3. Fabrication process for the microbattery. An adhesive bonds two wafers and creates a reaction chamber.

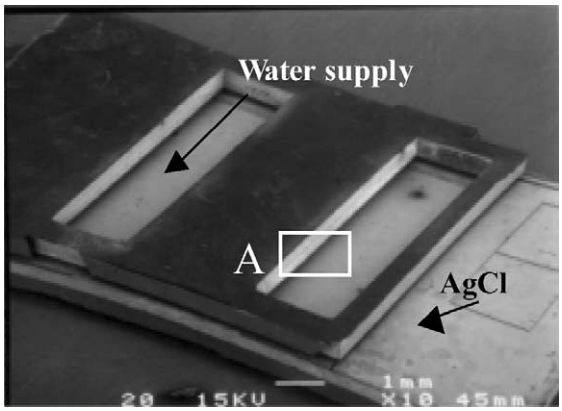

Fig. 4. SEM photograph of a fabricated microbattery: the electrode area is 8 mm × 8 mm.

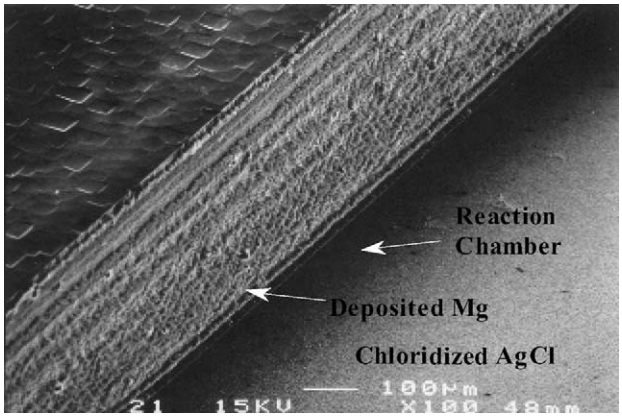

Fig. 5. Close view of Fig. 4 showing the chlorinated AgCl, gap of the reaction chamber and magnesium deposition on the sidewall of the top substrate.

4. Results and discussions

The output voltages of the microbatteries have been measured with respect to time under various discharge loads, electrode areas, cathode materials, and gap widths of the

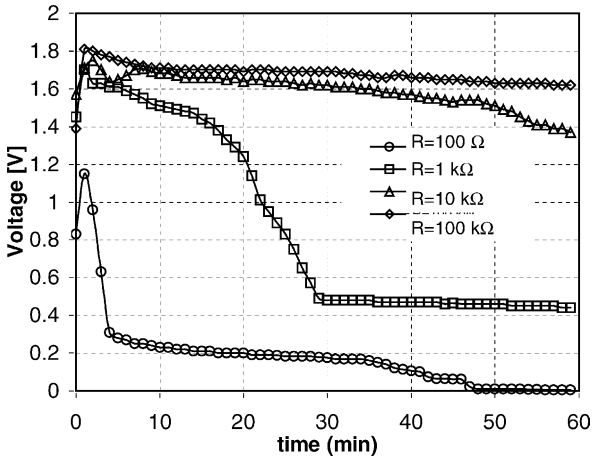

Fig. 6. Measured voltage of the 8 mm × 8 mm microbattery with AgCl as the cathode and a 100 μm-high chamber.

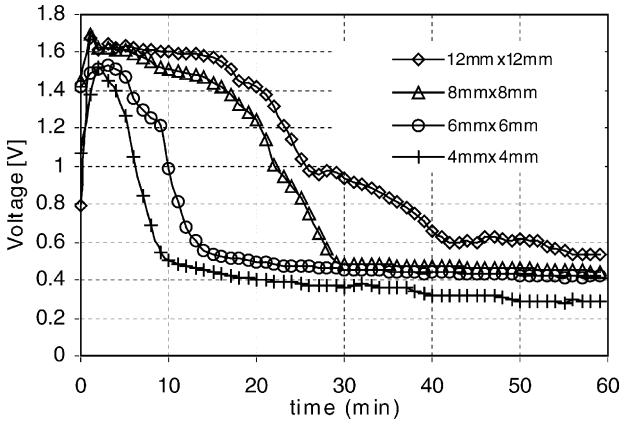

Fig. 7. Measured voltage of microbatteries with AgCl as the cathode and a 100 μm-high chamber discharged at 1 kΩ.

reaction chamber. Placing a droplet of water of about 40 μl in all experiments activated these microbatteries. Fig. 6 shows the measured voltages of an 8 mm × 8 mm microbattery that has a reaction chamber of 100 μm in height and uses AgCl as the cathode. When discharged at 1 kΩ, the voltage reached a maximum of 1.7 V after 1 min of operation and the value reduced to 0.46 V after 25 min and remained at about this value for the rest of the operation. As noted in Fig. 6, the measured voltage decreased with time and this is due to the chemical consumption within the batteries. Moreover, the voltage was lower when the batteries were discharged at a higher load resistance. The measured voltage, V_m could be approximately expressed as:

$$V_m = \frac{(E_0 + E_p)R}{R + R_i} \tag{9}$$

where E_0 is the theoretical voltage, E_p the voltage drop due to the reaction at the electrode/solution interface, R the load resistance, and R_i is the internal resistance. It could be deduced from Eq. (9) that as load resistance increases, discharge voltage increases. Fig. 7 shows the discharge curves under a 1 kΩ load resistor for various electrode areas with

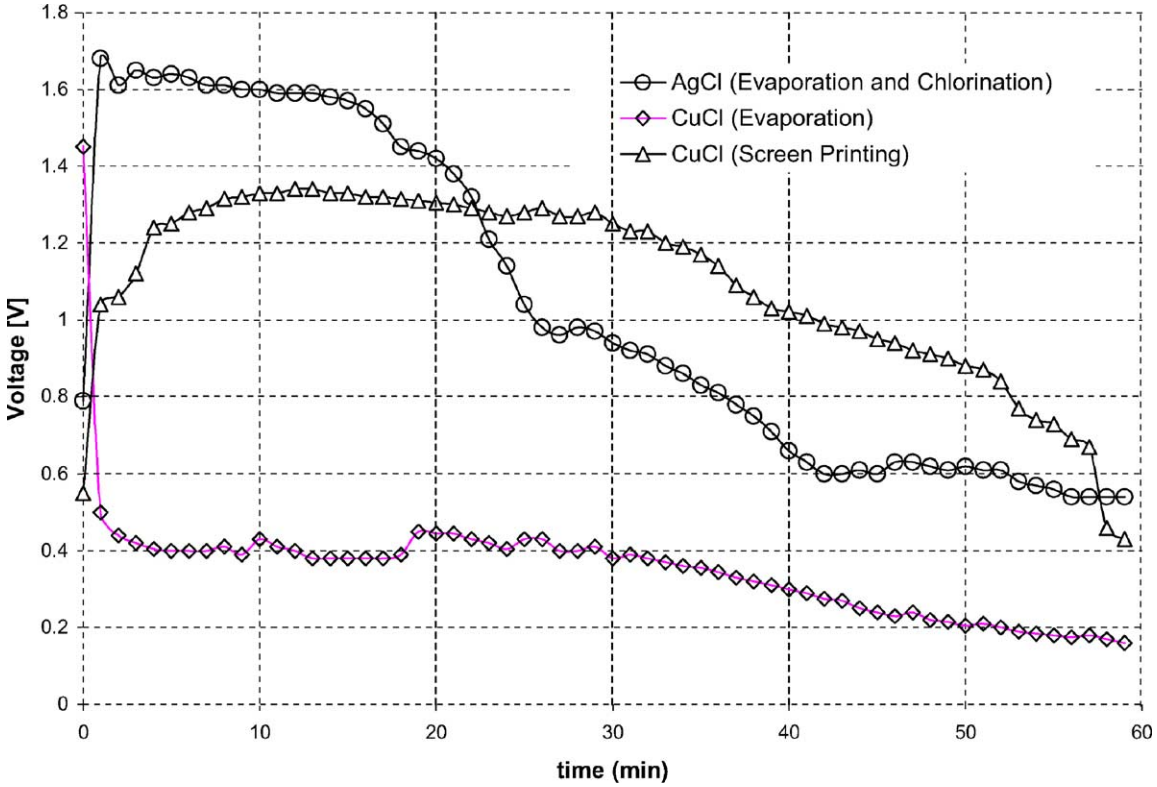

Fig. 8. Measured voltage of the 12 mm × 12 mm micro-battery with a 100 μm-high chamber discharged at 1 kΩ.

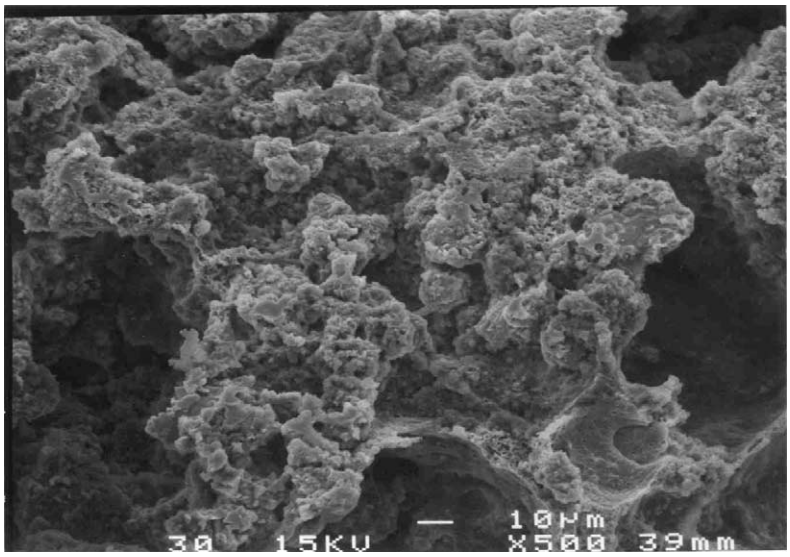

Fig. 9. SEM photograph of the screen-printed copper chloride (CuCl).

AgCl as the cathode and the chamber height is 100 μm. As shown in Fig. 7, the voltage decreases with electrode area because batteries with larger electrode areas have less internal resistance.

The performance of the microbattery for various cathode materials is compared in Fig. 8. The measured voltage of the AgCl microbattery was higher than that of the screen-printed CuCl for the first 22 min after which the measured voltage from the screen-printed CuCl microbattery was higher than that of the AgCl microbattery. Theoretically, CuCl microbatteries have lower output voltage than AgCl microbatteries (Table 2). In addition, screen-printed CuCl–Mg microbattery have a higher internal resistance in comparison to sputtered and chlorinated AgCl–Mg microbattery due to the presence of organic filler in the CuCl film. As a matter of fact, it would be theoretically expected that the discharge current of the AgCl microbattery would exceed that of screen-printed CuCl. This was the case for the first 22 min of discharge time. On the other hand, the rough topology of the screen-printed CuCl shown in Fig. 9 resulted in larger electrode area than that of evaporated and chlorinated AgCl. The latter was almost homogeneous as in shown Fig. 10. Moreover, the presence of pores within the screen-printed CuCl film helped in water penetrating the CuCl film that

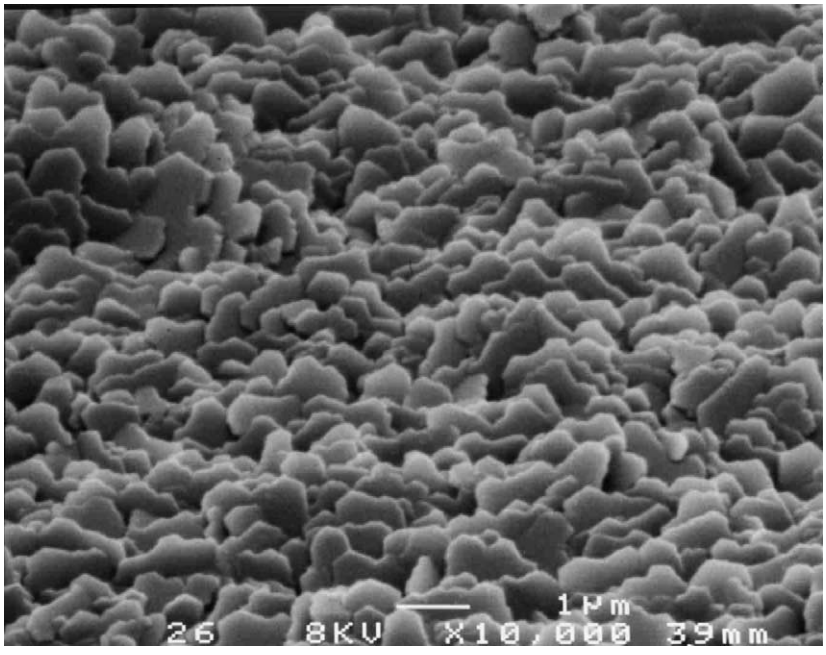

Fig. 10. SEM photograph of sputtered and chlorinated AgCl.

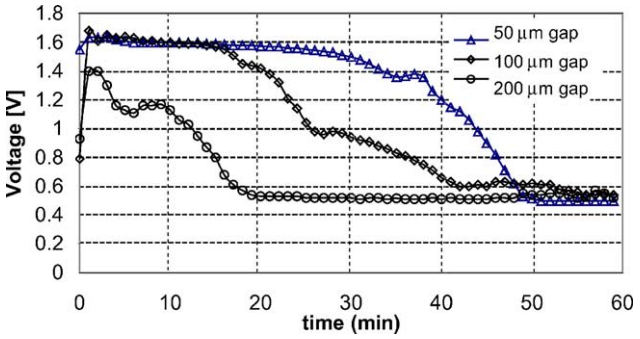

Fig. 11. Measured voltage of the 12 mm × 12 mm microbattery with AgCl discharged under a load resistor of 1 kΩ.

consequently increased the rate of electrons and ions within the chemical chamber. The higher cathode area and the presence of pores helped in sustaining the discharge current for the screen-printed CuCl microbattery for a prolonged period of time. The evaporated CuCl microbattery had an inferior performance in contrast to screen-printed CuCl because of the difference in film thickness as well as the unavoidable presence of Cu atoms within the CuCl film during the evaporation process that consequently decreased the effective cathode area. The energy capacity of AgCl–Mg microbattery with 12 mm × 12 mm electrode area and 100 μm reaction chamber height was 1266 μWh. The energy capacity of the screen-printed of CuCl–Mg microbattery with the same conditions as the AgCl microbattery was 1260.6 μWh, which is about the same as that of the tested AgCl–Mg microbattery. The energy capacity of the evaporated CuCl–Mg microbattery was 155.2 μWh, about one order of magnitude less than the other microbatteries presented in this work.

The effectiveness of the reaction chamber height on the performance of the microbattery has also been studied. Fig. 11 shows that the performance of the microbattery is enhanced as the height is reduced. As the gap between the cathode and anode is decreased, the resistance of the electrolyte within the reaction chamber is reduced. This results in a reduction in the internal resistance of the microbattery that consequently enhances the performance.

It is worth mentioning that hydrogen bubbles shown in Fig. 12 were observed at the outlet port during the testing of the microbatteries. The bubbles are direct outcome of the side chemical reaction between magnesium and water as indicated by Eq. (6). This reaction is disadvantageous in a sense that it will inevitably erode away the magnesium electrode that results in lowering the experimental voltage and energy capacity per unit mass of the microbattery to their

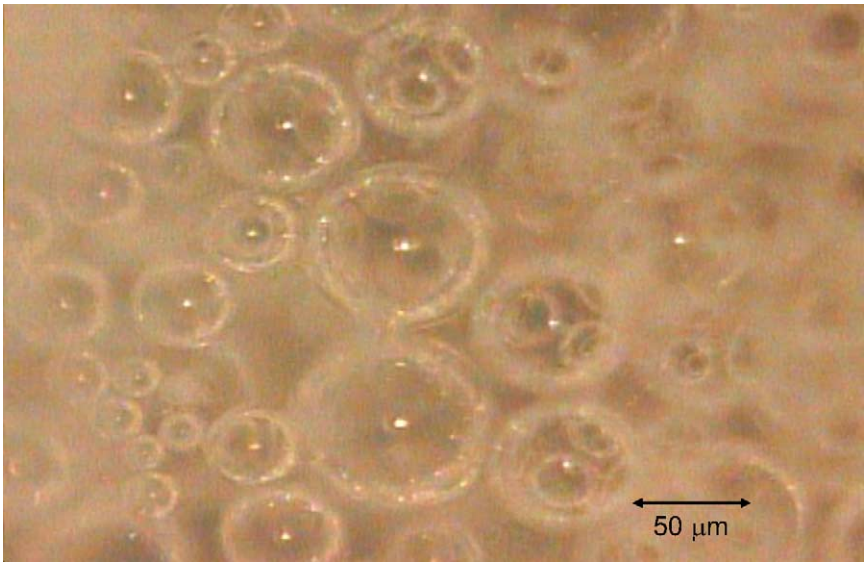

Fig. 12. A microscope picture of bubbles observed at the outlet port.

Table 3
Energy capacities from Figs. 6–8 and 11 in mWh

Electrode area (mm × mm)	Material	Gap (μm)	100 (Ω)	1 (kΩ)	10 (kΩ)	100 (kΩ)
12 × 12	AgCl	50	↔	1766.5		
12 × 12	AgCl	200	↔	543.6	↓	↓
12 × 12	AgCl	100	↔	1266.0		
8 × 8	AgCl	100	808.2	999.4	254.3	28.17
6 × 6	AgCl	100	↔	530.2		
4 × 4	AgCl	100	↔	337.4		
12 × 12	CuCl	100	↔	1260.6	←Screen printing	
12 × 12	CuCl	100	↔	155.16	←Evaporation	

respective theoretical values. On the other hand, the motion of the hydrogen bubbles throughout the reaction chamber to the outlet port is beneficial in pumping out the reaction byproducts such as $Mg(OH)_2$, $CuCl_2$, and $AgCl_2$ to outside the reaction chamber. Otherwise, the reaction byproducts would have deposited on the electrode surfaces and gradually blocked the reaction between the cathode and the anode.

Table 3 compares the experimental energy capacity calculated from the numerical integration of the data in Figs. 5–8. As noted from Table 3, the energy capacity increased from 543.6 μWh for chamber height of 200 μm to 1766.5 μWh for chamber height of 50 μm microbatteries.

5. Conclusions

We have successfully demonstrated a new class of on-demand, and disposable microbatteries based on a safe activation mechanism by using water. The manufacturing process only requires one mask and is compatible with most micromachining processes, including CMOS. The prototype demonstrations use magnesium as the anode and silver chloride or cuprous chloride as the cathode and other material systems may provide even better results. The experimental data have shown that a maximum output voltage of 1.65 V and energy capacity of 1.8 mWh is achieved for a microbattery with an electrode area of 12 mm × 12 mm when the reaction chamber gap separating the cathode and anode is 50 μm and the activation water droplet is 40 μl. Both reducing the reaction chamber height and increasing the electrode areas proved to provide higher voltage outputs. Furthermore, this work demonstrated that appreciable amount of energy can be extracted from the fabricated microbatteries with energy scaling up linearly with the electrode area. These microbattery might be easily integrated with microsystems to provide suitable power for various applications, including disposable diagnostics and BioMEMS chips.

Acknowledgements

This project is supported in part by a DARPA/DSO/BioFlips grant and these devices were fabricated in the UC–Berkeley Microfabrication Laboratory. The authors would like to thank Mr. Ron Wilson for taking the SEM pictures.

References

[1] M. Madou, Fundamentals of Microfabrication, CRC Press, Boca Raton, FL, 1997.
[2] L. Doherty, B.A. Warneke, B.E. Boser, K.S.J. Pister, Energy and performance considerations for smart dust, Int. J. Parallel Distributed Syst. Netw. 4 (3) (2001) 121–133, Acta Press.
[3] P.B. Koeneman, I.J. Busch-Vishniac, K.L. Wood, Feasibility of micro power supplies for MEMS, J. Microelectromech. Syst. (1997) 355–362.
[4] A.H. Epstein, S.D. Senturia, Micro power from micro machinery, Science 276 (1997) 1211.
[5] J.B. Lee, Z. Chen, M. Allen, A. Rohatgi, A miniaturized high-voltage solar cell array as an electrostatic MEMS power supply, J. Microelectromech. Syst. 4 (1995) 102–108.
[6] A. Mehra, X. Zhang, A. Ayon, I.A. Waitz, M.A. Schmidt, C.M. Spadaccini, A six-wafer combustion systems for a silicon micro gas turbine engine, J. Microelectromech. Syst. 9 (2000) 517–527.
[7] S.D. Jones, J.R. Akridge, A microfabricated solid-state secondary Li battery, Solid State Ionics 86–88 (1996) 1291–1294.
[8] K.B. Lee, L. Lin, Electrolyte based on-demand disposable microbattery, in: MEMS 2002 IEEE International Conference, Las Vegas, 2002, pp. 236–239.
[9] D. Linden, Handbook of Batteries, second ed., McGraw-Hill, New York, 1995.
[10] P.W. Atkins, General Chemistry, Scientific American Books, 1989.

Biographies

Firas Sammoura was born in Lebanon in 1980. He received his BE degree in mechanical engineering from the American University of Beirut (AUB) in 2001. He received his MS degree in mechanical engineering from the University of California at Berkeley in December 2002. He is currently working towards his PhD degree in the field of microelectromechanical systems at the University of California at Berkeley. His research interests include micropower generation devices, microactuators, as well as microsystems.

Ki Bang Lee was born in Korea in 1962. He received the BS, MS, and PhD degrees, all in mechanical engineering, from the Hanyang University, Seoul, Korea, and the Korea Advanced Institute of Science and Technology (KAIST), Korea, in 1985, 1987, and 2000, respectively. He worked with Samsung Advanced Institute of Technology (SAIT), Yonginsi, Korea during 1987–2000. With Samsung and KAIST, he worked on the projects on design and fabrication of micromirror and microactuator for data storage system and hard disk drive, microactuators for tuning frequency and quality factors, design and fabrication of microgyroscope, color printer and inkjet print head, simulation and measurement of air gap between the magnetic head and tape of video cassette recorder (VCR), and noise and vibration control for refrigerators. He has been a post-doctoral researcher of the Berkeley Sensors and Actuator Center (BSAC) at the University of California at Berkeley since November 2000. Since joining BSAC, he has been involved in the projects of Massively Parallel Post-Packaging for MEMS, Integrated Microwatt Transceivers and Water-Powered Bioassay Systems that are all supported by Defense Advanced Research Projects Agency (DARPA). His research interests include microelectromechanical systems (MEMS); bioMEMS; micropower generation including disposable microbattery; design and fabrication of microsensors and microactuators; integrated disposable microsystems such as DNA chips, diagnostic devices, and/or labs-on-a-chip with disposable micropower; microvehicles for MEMS/bioMEMS application; microfluidic devices.

Liwei Lin (S'92–M'93) received the MS and PhD degrees in mechanical engineering from the University of California at Berkeley in 1991 and 1993, respectively. From 1993 to 1994, he was with BEI Electronics, Inc., USA, in research and development of microsensors. From 1994 to 1996, he was an associate professor in the Institute of Applied Mechanics, National Taiwan University, Taiwan. From 1996 to 1999, he was an assistant professor at the Mechanical Engineering and Applied Mechanics Department at the University of Michigan, Ann Arbor. In 1999, he joined the University of California at Berkeley and is now an associate professor at Mechanical Engineering Department and co-director at Berkeley Sensor and Actuator Center, NSF/Industry/University research cooperative center. His research interests are in design, modeling, and fabrication of microstructures, microsensors, and microactuators as well

as mechanical issues in microelectromechanical systems including heat transfer, solid/fluid mechanics, and dynamics. He holds eight US patents in the area of MEMS. Dr. Lin is the recipient of the 1998 NSF CAREER Award for research in MEMS Packaging and the 1999 ASME Journal of Heat Transfer Best Paper Award for his work on microscale bubble formation. He served as chairman of the Micromechanical Systems Panel of the ASME Dynamic Systems and Control Division in 1997 and 1998 and led the effort in establishing the MEMS subdivision in ASME and is currently the vice chairman of the Executive Committee.